The final version of this manuscript appeared in the Proc. of the IEEE International Conference on Communications (ICC 2015)
June 8-12, 2015, London, GB
DOI: not yet available

Transmitting information with microfluidic systems

Andrea Biral, Davide Zordan, Andrea Zanella
Department of Information Engineering, University of Padova, Italy
E-mail: {biraland, zordanda, zanella}@dei.unipd.it

***Abstract*—In recent past, researchers have suggested the idea of extending information theory to the microfluidic domain. Along this stream, a few solutions have been proposed to support logic and computing functions as well as simple communications in droplet-based microfluidic systems. Of course, pursuing this objective, requires a deep knowledge of microfluidic basics and relies on the use of an appropriate information coding strategy. Accordingly, in this paper we introduce a possible scheme for information coding in microfluidic devices, evaluate its performance by means of some preliminary experimental results and draw a number of considerations.**

***Index Terms*—Droplet-based microfluidics, T-junction, droplet generation, Pulse Amplitude Modulation, experiments.**

I. Introduction

Microfluidics is both a science and a technology that deals with the control of small amounts of fluids flowing through microchannels. These have dimensions in the order of micrometers and are usually fabricated in PDMS, i.e., Polydimethylsiloxane, which is a silicon based organic polymer. In this paper we are specifically interested in the so called *droplet-based microfluidic* which is a branch of microfluidics related to the control of droplets in such microchannels. In this scenario, small drops of a certain fluid are dispersed into another immiscible fluid: in literature the first fluid is conventionally called *dispersed phase*, while the second is called *continuous phase*. This line of reserch has emerged strongly in the past few years, but the field is still at an intermediate stage of development. Nevertheless its capabilities and advantages are already well known. The microfluidic technology, in fact, exploits both its most obvious characteristic (small size) and less obvious characteristics of fluids in microchannels (such as laminar flow) to provide new capabilities in the control and concentrations of molecules in space and time. Moreover it has the potential to influence many subject areas, from chemical synthesis and biological analysis to optics and information technology [1], [2], [3].

Focusing on this last aspect, physics researchers have advanced the idea of exploiting microfluidic systems to build tiny computing units [4], [5], and the possibility of using them in order to realize simple boolean functions has been experimentally proved. Even more interesting is the recent proposal of introducing communication notions in the microfluidic domain: a preliminary step in this direction was done in [6], [7], where the authors proposed to encode information in the distance between consecutive drops.

Inspired by these works, we carried out some experiments using real microfluidic devices with the intent of investigating a proper way to transmit information in a microfluidic channel. In particular, we exploited the T-junction droplet generator governing laws in order to modulate the length of generated droplets (and, consequently, their interdistance) in a sort of binary Pulse Amplitude Modulation scheme.

In Sec. II we introduce the main physics phenomena at the basis of microfluidics. Then, in Sec. III we will present the setting, describe the method and show the results obtained in our experiments. Moreover, such outcomes will be technically analyzed in order to study their implications as far as information encoding is concerned and, thus, to formalize our communication scheme. Finally, in Sec. IV we will draw our concluding remarks.

II. Microfluidic basics

The aim of this section is to let the reader familiarize with the principal concepts of microfluidics, which will be recalled and exploited throughout the entire work. In particular, we focus on the droplet generation mechanism since it is at the basis of our communication scheme. For further details concerning microfluidic issues, please refer to [8], [9].

First of all, according to the Hagen-Poiseuille equation, the average volumetric rate Q_c in a microfluidic channel of length L, filled with a generic fluid with dynamic viscosity μ_c, is proportional to the pressure gradient ΔP through the law

$$\Delta P = R(\mu_c, L)\, Q_c \,, \tag{1}$$

where, in analogy to the Ohm's law for electrical circuits, the parameter $R(\mu_c, L)$ is called *fluidic resistance*. In general, $R(\mu_c, L)$ can be expressed as [10]

$$R(\mu, L) = \frac{a\mu L}{wh^3} \,, \tag{2}$$

where a is a dimensionless parameter that depends on the channel geometry and, for rectangular sections, equals

$$a = 12 \left[1 - \frac{192h}{\pi^5 w} \tanh\left(\frac{\pi w}{2h}\right) \right]^{-1} . \tag{3}$$

However, when a droplet is injected into a duct, the friction generated with the carrier fluid and the forces produced by the inhomogeneity between the dynamic viscosity of the continuous and dispersed phases determine a change of the hydraulic resistance of the channel [11], [12], [13]. Mathematically, the *variation* of resistance produced by a droplet of length ℓ_d in

a channel of length L can then be approximated as [9]

$$\begin{aligned}\rho(\ell_d) &= R(\mu_c, L-\ell_d) + R(\mu_d, \ell_d) - R(\mu_c, L) \\ &= (\mu_d - \mu_c)\frac{\ell_d a}{wh^3}\,,\end{aligned} \tag{4}$$

so that the overall fluidic resistance of the channel when crossed by a droplet of length ℓ_d is $R(\mu_c, L)+\rho(\ell_d)$. Note that, these relations are (approximately) verified in practice only when the droplet is large enough to entirely fill the channel section, with an extremely thin stream of continuous phase between the droplet and the channel surfaces. In this case, the speed of the droplet when crossing a channel is basically the same as that of the continuous phase in that channel, i.e.,

$$u_d = u_c = \frac{Q_c}{wh} = \frac{\Delta P}{wh(R(\mu_c, L) + \rho(\ell_d))}\,; \tag{5}$$

where Q_c is the volumetric flow rate of the continuous phase in the channel, and ΔP is the pressure gradient between the endpoints of the channel.

A. Droplet generation

As said before, our final aim in this paper is to provide a communication scheme for microfluidic systems based on the modulation of the droplets length/interdistance. As such, an essential aspect to be analyzed is the method for generating droplets in a controlled fashion. Not only should these devices produce a regular and stable monodisperse droplet stream, they also need to be flexible enough to easily provide droplets of prescribed volume at prescribed rates. To this end, three main approaches have emerged so far [14], based on different physical mechanisms:

- breakup in co-flowing streams;
- breakup in elongational strained flows (flow focusing devices);
- breakup in cross-flowing streams (T-junction).

We focus only on the last one, which is the most appropriate solution in our case since it is well suited for planar geometries and has clear-cut scaling laws for its physical behavior.

Fig. 1 illustrates the geometry of such a T-junction droplet generator. Very simply, it consists of two channels merged at right angle. The main channel carries the continuous (or carrier) fluid and the orthogonal channel supplies the fluid that will be dispersed in droplets. The channels have rectangular cross sections, and there are only three geometrical parameters that define completely the size and shape of the T-junction: the width w_c of the main channel, the width w_d of the channel supplying the dispersed fluid, and the height *h* of the channels. In this regard, we focus on planar geometries, with identical rectangular cross-section for every channel, in which the width is slightly greater than the height. Liquid flows are commonly controlled via independent syringe pumps imposing the inlet volumetric flow rates Q_c and Q_d for the continuous and dispersed phase respectively.

The process of droplet formation begins as soon as the dispersed phase starts penetrating into the outer channel. Here, three main forces act on the emerging interface and influence

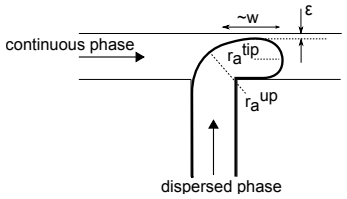

Fig. 1. Example of droplet production in a T-junction (top view).

droplet breakup: the surface (or interfacial) tension force (F_σ), which has a stabilizing effect, and the viscous shear-stress force (F_τ) and squeezing force (F_S),[1] both of which have a destabilizing effect and, eventually, lead to the breakup of droplets from the dispersed liquid.

As stated by several studies [15], [16], [17], the balance of these forces causes two principal regimes of breakup:

- *squeezing regime*, characterized by the stable formation of uniform and evenly spaced droplets;
- *dripping regime*, where the balance of the forces is much more unstable and short droplets are generated before they can block the main channel.

Importantly, the transition between them is governed by the Capillary number (Ca), which is a dimensionless parameter that describes the relative magnitude of the viscous shear stress compared with the interfacial tension. A simple definition for Ca in microfluidics is given in terms of the average velocity u_c of the continuous phase, the dynamic viscosity μ_c of the continuous phase and the interfacial tension coefficient σ [18]:

$$Ca = \frac{\mu_c u_c}{\sigma} = \frac{\mu_c Q_c}{\sigma w h}. \tag{6}$$

In particular, for low values of the Capillary number ($Ca < Ca^*$), i.e., when the interfacial forces dominate the shear stress, the dynamics of breakup of immiscible thread in T-junction is dominated by the squeezing force across the droplet as it forms (squeezing regime). In the opposite case ($Ca > Ca^*$), the shear stress starts playing an important role and the system starts operating in the so called dripping regime. As reported in a recent paper [16] and confirmed in our numerical simulations, this threshold is given by:

$$Ca^* \approx 10^{-2}. \tag{7}$$

Let us now examine in more detail the regimes mentioned above with a particular focus on the squeezing regime, which is the one we will adopt later on for our microfluidic communication system because it shows the best flexibility and controllability over the shape of generated droplets.

a) Squeezing regime: The typical process of droplets formation via squeezing regime is visually depicted in the simulation of Fig. 2, obtained with OpenFOAM software, where the principal geometric and physical parameters are the following: $h = 50\,\mu m, w_c = w_d = 150\,\mu m, Q_c = 3.75\,nL/s, Q_d = 1.875\,nL/s$. Keeping in mind the previous

[1]This force arises from the increased resistance to flow of the continuous fluid around the tip of droplet that is being formed.

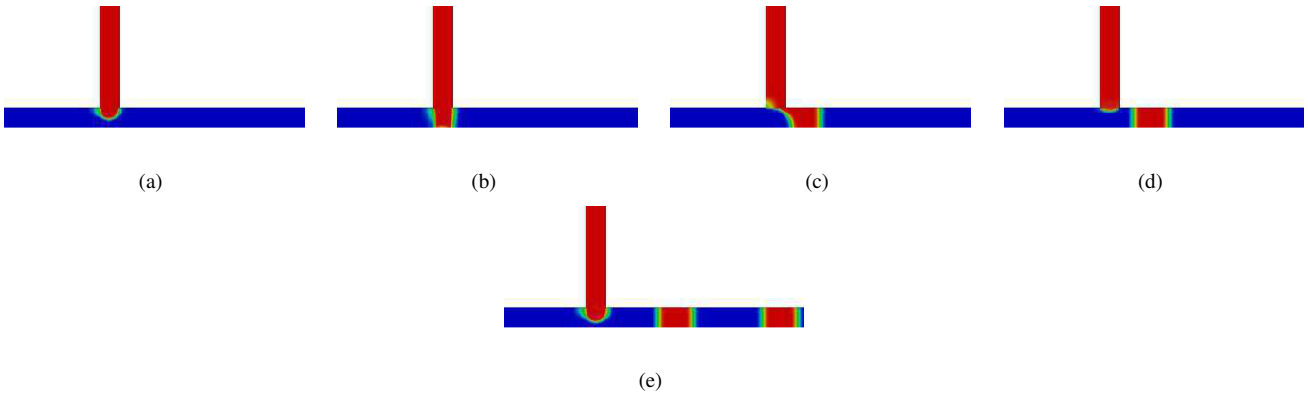

Fig. 2. Typical process of droplet formation in squeezing regime.

analysis and observations, the droplet generation mechanism can be briefly described as follows: the two immiscible fluids form an interface at the junction of the dispersed inlet channel with the main channel. The stream of the discontinuous phase starts penetrating into the main channel and a droplet begins to grow under the effect of the viscous shear-stress force (Fig. 2(a)). The latter, however, is not sufficient to distort the interface significantly because this operating regime works under the condition $Ca < Ca^*$, so that interfacial tension dominates shear stress. Consequently, the emerging droplet manages to fill the junction and restricts the available area through which continuous fluid can pass, leading to an increased pressure directly upstream of the junction (Fig. 2(b)). When the corresponding squeezing force overcomes the interfacial tension force, the neck of the emerging droplet squeezes (Fig. 2(c)), promoting its breakup. Finally, the disconnected liquid plug flows downstream of the main channel, while the tip of the dispersed phase retracts to the end of the inlet and the process repeats itself anew (Fig. 2(d)). The intrinsic high reproducibility shown by this mechanism is fundamental for the stable production of uniform droplets with identical length and shape (Fig. 2(e)) over a wide range of flow rates. This is also the reason why we chose to work under squeezing regime in our simulations of T-shaped droplet inlet systems.

b) Droplets length: Garstecki *et al.*[16] obtained a simple formula for the length L_d of the droplets resulting from breakup at the T-junction in the squeezing regime, i.e.,

$$L_d = w(1 + \xi \frac{Q_d}{Qc}) \; ; \tag{8}$$

where w is the width of the main channel, Q_d is the flow of the dispersed phase, Q_c is the flow of the carrier fluid and ξ is a dimensionless parameter that depends on the geometric and physical parameters of the system. Eq. (8) can be intuitively explained by considering that detachment begins when the emerging discontinuous thread fills completely the main channel, i.e., when the squeezing force is stronger. At this moment, the length of the droplet is approximately equal to the width of the channel w, and the thickness of the neck in the junction starts decreasing at a rate that depends on the speed of the continuous flow u_c. The flow of the carrier fluid ($Q_c = u_c hw$), hence, determines the "squeezing time" necessary for the neck of the droplets to break. In fact, for a given dispersed phase flow, the greater the continuous flow the lower the squeezing time and thus the length of the resulting droplets. On the other hand, there is a direct proportionality between droplet length and dispersed phase flow ($L_d \propto Q_d$) because Q_d determines how much dispersed fluid forms a droplet before breakup.

c) Interdistance between droplets: Another physical parameter to be considered, is the spacing $\delta\,[m]$ between droplets generated in squeezing regime. Its scaling relation can be deduced from the application of the mass conservation law, as reported below.

Let us consider a sufficiently long time τ and the related distance $x = u'_d \tau$ covered by the droplets along the main channel, being u'_d the speed of the dispersed fluid in the main channel. The number of droplets generated in the time interval τ is given by:

$$n_d(\tau) = \frac{x}{L_d + \delta} = \frac{u'_d \tau}{L_d + \delta}, \tag{9}$$

where L_d is the length of each single droplet, and δ is the interdistance between droplets.

Beacuse of the mass conservation law, the volume of dispersed liquid injected by the discontinuous phase inlet channel throughout the time interval τ must correspond to the volume of dispersed fluid along x in the main channel, i.e.,

$$u_d wh\tau = \frac{V_d u'_d \tau}{L_d + \delta} \; ; \tag{10}$$

where V_d is the volume of the droplets. Accordingly:

$$\delta = \frac{V_d u'_d \tau}{u_d wh\tau} - L_d; \tag{11}$$

This general expression can be further specialized under some simplifying assumptions. First of all, we can make the hypothesis, confirmed by our simulations, that dispersed and continuous phase flow at the same velocity, i.e., $u'_d = u'_c = u$, though it is not always true[4]. Accordingly, by applying flows

conservation, we get:

$$Q = Q_d + Q_c \Rightarrow u = u_d + u_c.^2 \tag{12}$$

Substituting (12) in (10), it results:

$$u_d(L_d + \delta) = V_d(u_d + u_c). \tag{13}$$

Now, concerning the volume of the droplets, we notice that they are not exact parallelograms but are curved at the edges. Therefore, if we approximate the tips as hemispheres with radius $w/2$ we obtain:

$$V_d = wh(L_d - w) + \frac{1}{6}\pi w^3. \tag{14}$$

Putting all the pieces together, we obtain the following expression of the interdistance between droplets generated in a T-junction in the squeezing regime:

$$\begin{aligned} \delta &= \frac{V_d}{Q_d wh}(Q_d + Qc) - L_d \\ &= L_d \frac{Q_c}{Q_d} + \frac{\left(1/6\pi w^3 - w^2 h\right)}{Q_d wh}(Q_d + Q_c). \end{aligned} \tag{15}$$

Lingering on (15), it can be noted that droplets length and interdistance are correlated since δ depends on L_d. Consequently, once fixed the geometry of the system and the physical parameters of the liquids, droplets with a specific length will have a corresponding precise interdistance between them.

In real microfluidic systems, however, the imperfections in the fabrication process, the non-ideal hardware, and the external interferences introduce variability in the results, as discussed in the next section.

III. Results

As we said in the introduction, our aim is to design a microfluidic communication system in which the information is encoded in the droplets length/interdistance. To this end, we considered a 4-levels modulation scheme with symbols $s^{(i)}$, $i \in \{0, 1, 2, 3\}$, which are associated, respectively, to the bit strings $\{00, 01, 10, 11\}$. For each symbol we set a different level for the dispersed phase flow $Q_d^{(i)}$ in order to obtain different droplet lengths $L_d^{(i)}$ and interdistances $\delta^{(i)}$ as per (8) and (15). The continuous phase flow Q_c is fixed. We then investigate the performance of a T-junction in generating trains of droplets with a given size and interdistances.

To this end we designed and realized a basic microfluidic circuit, used for the experiments. Next, we describe the experimental setup, characterizing the microfluidic chip, the fluids and the hardware used. Thus we show the experimental results on the droplet generation process. Finally we assess the symbol error probability for a PAM–like system in which modulation is realized by exploiting the droplet length/interdistance, and we discuss the challenges and the performance tradeoffs of such a system.

[2]The last implication follows from the fact that we always consider channels with identical cross section.

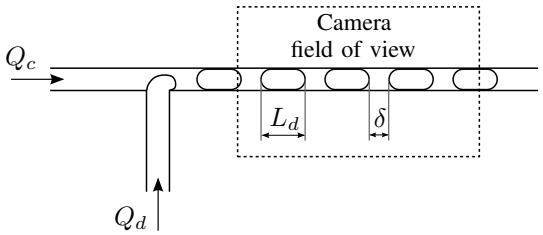

Fig. 3. Sketch of the experimental setup.

A. Experimental setup

The microfluidic device we considered for our experiments is a T-junction droplet generator. The device, made of polydimethylsiloxane (PDMS), was fabricated using the photolithography technique. We designed the chip with channels of height $90\,\mu m$ and width $115\,\mu m$. The continuous and the dispersed phase are injected in the system through two PHD 2000 Harvard Apparatus syringe pumps, while the output channel opens on air.

The continuous phase is a solution of Hexadecane, an alkane hydrocarbon, and Span® 80, a nonionic surfactant that lowers the surface tension. The dispersed phase is instead an Aqueous Glycerol solution (Glycerol 60% weight/weight).

We used a camera connected to a microscope to record real-time videos of the experiments (see *www.youtube.com/channel/UCSAv6jxxZq4xmmFSpNKyoSw*). The camera takes 20 frame per second, for a time duration of 50 seconds for each experiment. The camera field of view is centered on a section of the output channel of the T-junction, as shown in Fig. 3. Hence, the droplet length/interdistance are obtained from the acquired frames through an image processing script.

B. Droplet generation

We set the continuous phase flow $Q_c = 5\,\mu l/\mathrm{min}$, whereas the dispersed phase phase flow $Q_d^{(i)}$ takes values in the set $\{0.5, 1, 1.5, 2\}\,\mu l/min$, for symbols $s^{(i)}$, $i \in \{0, 1, 2, 3\}$ respectively. For each value of $Q_d^{(i)}$ the system is left running for a sufficiently long time. The camera connected to the microscope acquires 1000 frames, which are post processed to obtain the values for $L_d^{(i)}$ and $\delta^{(i)}$ in the 50 s acquisition time interval. Fig. 4 and Fig. 5 show the results, obtained through image processing, for $L_d^{(i)}$ and $\delta^{(i)}$. It can be noted that there are non negligible fluctuations around the average values. Tab. I reports the mean value, as well as the standard deviation for both the droplet lengths and the interdistances. Specifically, we define $\bar{L_d}^{(i)}$ and $\sigma_d^{(i)}$ as the average droplet length and the standard deviation for the i-th symbol respectively. Similarly, $\bar{\delta}^{(i)}$ and $\sigma_\delta^{(i)}$ indicate the average interdistance and the standard deviation of the droplets interdistance for the i-th symbol.

C. Symbol Error Probability

In order to evaluate the performance of the microfluidic communication system we assume that, for each symbol, the length/interdistance can be modeled as a Gaussian random

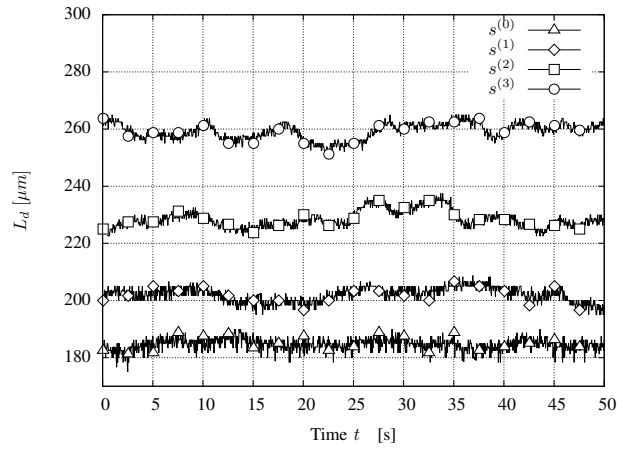

Fig. 4. Droplet lengths for the four experimental setup considered.

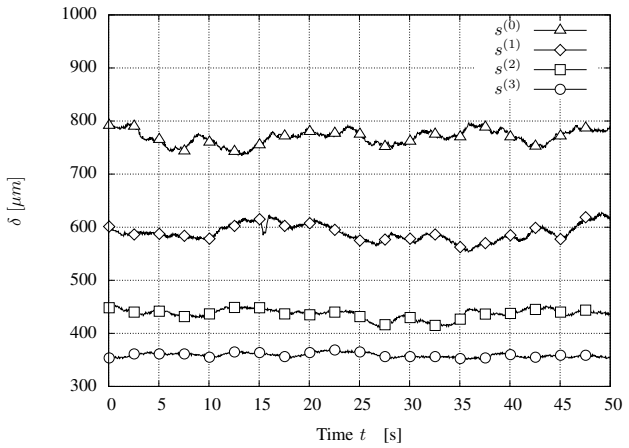

Fig. 5. Droplet interdistances for the four experimental setup considered.

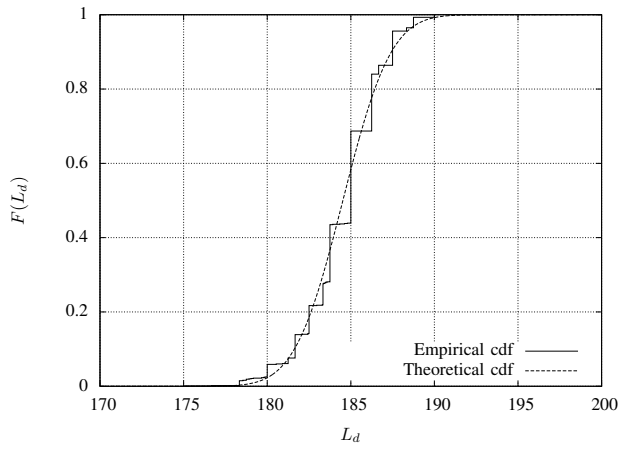

Fig. 6. Empirical and theoretical cdfs of the droplet length for symbol $s^{(0)}$.

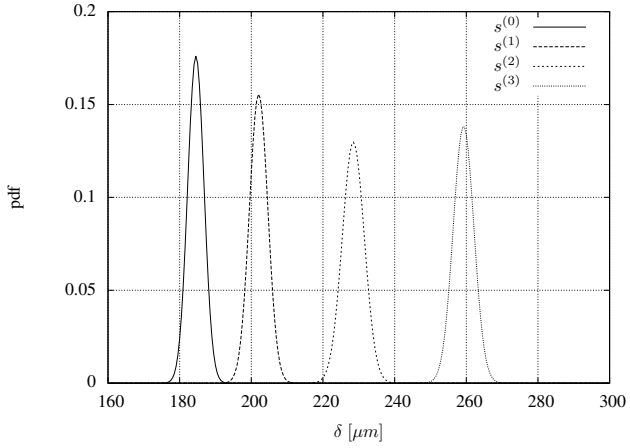

Fig. 7. Estimated pdfs of the four symbols when using droplet length modulation.

variable $\mathcal{N}^{(i)}(\mu_i, \sigma_i^2)$, where $\mu_i \in \{\bar{L}_d^{(i)}, \bar{\delta}^{(i)}\}$ and $\sigma_i \in \{\sigma_d^{(i)}, \sigma_\delta^{(i)}\}$ depending on whether we consider the length of the droplets or their inter-distance as the modulating quantity. Although further analysis is needed, the normal approximation for these quantities appears reasonable, as qualitatively proved by Fig. 6 that shows the empirical cdf of the droplet length for symbol $s^{(0)}$, as well as the theoretical normal cdf. As it can be seen, the theoretical curve approximates tightly the empirical cdf. The same assumption holds also for the other symbols, and for the distribution of the interdistances.

TABLE I
NUMERICAL RESULTS FOR THE DROPLET LENGTHS, INTERDISTANCES, DECISION THRESHOLDS AND TOTAL SYMBOL ERRORS IN THE FOUR EXPERIMENTAL SETUP CONSIDERED .

i	$\bar{L}_d^{(i)}$	$\sigma_d^{(i)}$	$\mathrm{thr}_L^{(i,i+1)}$	$\bar{\delta}^{(i)}$	$\sigma_\delta^{(i)}$	$\mathrm{thr}_\delta^{(i,i+1)}$
0	184.52	2.26	193.29	769.65	14.04	679.5107
1	202.05	2.56	215.26	589.37	15.30	513.0877
2	228.47	3.08	243.85	436.80	9.44	397.8275
3	259.24	2.88	/	358.85	4.09	/
e_L	$1.80 \cdot 10^{-5}$			e_δ	$8.95 \cdot 10^{-7}$	

Given the Gaussian random models, we identify the decision thresholds for the decoding of the symbols at the receiver of the microfluidic communication system as:

$$\mathrm{thr}_L^{(i,i+1)} = \frac{\bar{L}_d^{(i)} + \bar{L}_d^{(i+1)}}{2} \ , \ i \in \{0, 1, 2\} \ ; \qquad (16)$$

for the droplet lengths. Correspondingly we use $\bar{\delta}^{(i)}$ for the evaluation of the thresholds for the interdistance case, $\mathrm{thr}_\delta^{(i,i+1)}$. The values of the decision thresholds are reported in Tab. I

Fig. 7 and Fig. 8 show the probability distribution functions (pdfs) for the droplet lengths and the interdistances. It can be noted that in both cases the pdfs of different symbols are sufficiently spaced apart and that the overlapping between pdfs is minimal.

Following the standard procedure for a PAM-like modulation system, the error probability is derived by first computing

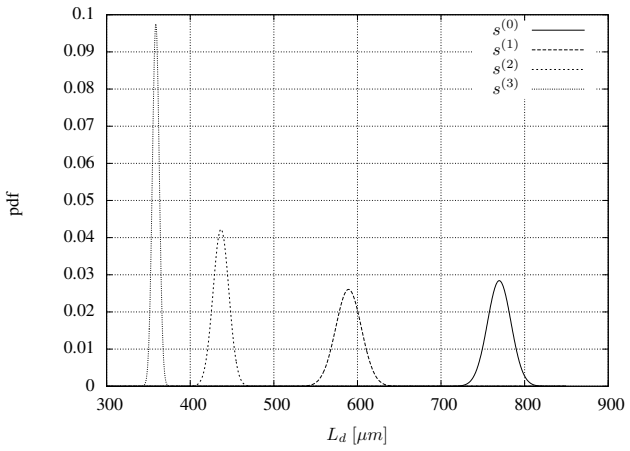

Fig. 8. Estimated pdfs of the four symbols when using droplet interdistance modulation.

the conditional probabilities of error and then applying the total probability theorem. Assuming equally likely symbols, we have:

$$e = \frac{1}{4}\sum_{i=0}^{3} P(E|s^{(i)}) \,, \tag{17}$$

where $P(E|s^{(i)})$ is the conditional probability of error when symbol $s^{(i)}$ is transmitted, and it is obtained using the decision thresholds and the symbol pdf. The last row of Tab. I summarizes the results for the error probability when using the droplet length, e_L, or the droplets interdistance, e_δ, as the modulating variable.

IV. Discussion

In this paper we investigated the feasibility of extending communication concepts to the microfluidic domain. We started by illustrating the main notions of droplet generation, and discussed their possible use to implement basic modulation techniques in microfluidic systems. On this basis, we carried out some experiments in order to investigate simple communication solutions in microfluidic channels using droplet length and interdistance modulation.

Results show that the noise that affects both droplet length and inter-distance can be modeled as a zero-mean normal random process, whose variance, however, depends on the transmitted symbol, i.e., on the working point of the system. More specifically, droplet-based modulation exhibits stronger noise for symbols associated to relatively short droplets, while interdistance-based modulation is more noisy when droplets are more spaced apart. Overall, however, droplet interdistance appears to be more robust a signal than droplet length for PAM modulation, though both techniques can achieve relatively low bit error probability in the considered scenarios. Although this analysis moves some initial steps toward the performance characterization of a microfluidic-based PAM transmission system, the way to go is still very long and unexplored. To begin with, the impact of the hardware used in the experiments shall be characterized, in order to sort out the microfluidics effects from other sources of noise. As an example, the transient exhibited by the droplet generation circuit when changing the volumetric flow rates at the input has not yet been analyzed, nor has it been considered the actual bitrate that can be achieved with such a mechanism. To this end, we are planning to carry out further experiments that will hopefully shed light on these and other aspects.

V. Acknowledgements

This work has been partially funded by the University of Padova project "Microfluidic Networking (MiNET): introducing networking technologies in microfluidic systems". The fabrication of the microfluidic circuit and realization of the experiments were made possible thanks to the precious collaboration with the Physics department of the University of Padova, which kindly made its labs, human resources and instruments available for the cause. In this regard, our most sincere thanks go to Prof. Giampaolo Mistura and PhD Students Enrico Chiarello and Paolo Sartori.

References

[1] P. S. Dittrich and A. Manz, "Lab-on-a-chip: microfluidics in drug discovery," *Nature Reviews Drug Discovery*, vol. 5, pp. 210–218, Mar. 2006.

[2] A. Huebner, S. Sharma, M. Srisa-Art, F. Hollfelder, J. B. Edel, and A. J. Demello, "Microdroplets: a sea of applications?" *Lab on a Chip*, vol. 8, pp. 1244–1254, Aug. 2008.

[3] L. K. Chin, A. Q. Liu, J. B. Zhang, C. S. Lim, and Y. C. Soh, "An on-chip liquid tunable grating using multiphase droplet microfluidics," *Applied Physics Letters*, vol. 93, no. 16, 2008.

[4] M. J. Fuerstman, P. Garstecki, and G. M. Whitesides, "Coding/Decoding and Reversibility of Droplet Trains in Microfluidic Networks," *Science*, vol. 315, no. 5813, pp. 828–832, 2007.

[5] M. Prakash and N. Gershenfeld, "Microfluidic Bubble Logic," *Science*, vol. 315, no. 5813, pp. 832–835, 2007.

[6] E. De Leo, L. Galluccio, A. Lombardo, and G. Morabito, "On the feasibility of using microfluidic technologies for communications in Labs-on-a-Chip," in *IEEE International Conference on Communications (ICC)*, Jun. 2012, pp. 2526–2530.

[7] ——, "Networked Labs-on-a-Chip (NLoC): Introducing networking technologies in microfluidic systems," *Nano Communication Networks*, vol. 3, no. 4, pp. 217–228, 2012.

[8] A. Biral and A. Zanella, "Introducing purely hydrodynamic networking mechanisms in microfluidic systems," in *IEEE International Workshop on Molecular and Nanoscale Communication (IEEE MoNaCom), Budapest, Hungary*, Jun. 2013, pp. 798–803.

[9] ——, "Introducing purely hydrodynamic networking functionalities into microfluidic systems," *Nano Communication Networks*, vol. 4, no. 4, pp. 205–215, 2013.

[10] M. J. Fuerstman, A. Lai, M. E. Thurlow, S. S. Shevkoplyas, H. A. Stone, and G. M. Whitesides, "The pressure drop along rectangular microchannels containing bubbles," *Lab Chip*, vol. 7, pp. 1479–1489, 2007.

[11] A. A. Carlson, M. Do-Quang, and G. Amberg, "Droplet dynamics in a bifurcating channel," *International Journal of Multiphase Flow*, vol. 36, no. 5, pp. 397–405, 2010.

[12] D. R. Link, S. L. Anna, D. A. Weitz, and H. A. Stone, "Geometrically mediated breakup of drops in microfluidic devices," *Phys. Rev. Lett.*, vol. 92, p. 054503, Feb. 2004.

[13] A. M. Leshansky and L. M. Pismen, "Breakup of drops in a microfluidic T junction," *Physics of Fluids*, vol. 21, no. 2, 2009.

[14] C. N. Baroud, F. Gallaire, and R. Dangla, "Dynamics of microfluidic droplets," *Lab Chip*, vol. 10, pp. 2032–2045, 2010.

[15] T. Thorsen, R. Roberts, F. H. Arnold, and S. R. Quake, "Dynamic pattern formation in a vesicle-generating microfluidic device," *Physical Review Letters*, vol. 86, no. 18, pp. 4163–4166, Apr. 2001.

[16] P. Garstecki, M. J. Fuerstman, H. A. Stone, and G. M. Whitesides, "Formation of droplets and bubbles in a microfluidic T-junction-scaling and mechanism of break-up," *Lab Chip*, vol. 6, pp. 437–446, 2006.
[17] M. de Menech, P. Garstecki, F. Jousse, and H. A. Stone, "Transition from squeezing to dripping in a microfluidic T-shaped junction," *Journal of Fluid Mechanics*, vol. 595, pp. 141–161, 2008.
[18] A. Gupta and R. Kumar, "Flow regime transition at high capillary numbers in a microfluidic T-junction: Viscosity contrast and geometry effect," *Physics of Fluids*, vol. 22, no. 12, 2010.